Geomechanics and Engineering, *Vol. 39, No. 5 (2024) 503-512*
https://doi.org/10.12989/gae.2024.39.5.503

Seismic stability of MSE walls with stepped reinforcement arrangement subjected to vertical and horizontal accelerations

Weichao Liu[1a], Peng Xu*[2], Guangqing Yang[1b] and Miren Rong[3c]

[1]*Department of Civil Engineering, Shijiazhuang Tiedao University, 17 Northeast Second Inner Ring, China*
[2]*State Key Laboratory of Mechanical Behavior and System Safety of Traffic Engineering Structures, Shijiazhuang Tiedao University, 17 Northeast Second Inner Ring, China*
[3]*School of Urban Geology and Engineering, Hebei GEO University, No. 136 East Huai'an Road, Yuhua Distirict, China*

(*Received August 24, 2023, Revised October 23, 2024, Accepted November 28, 2024*)

Abstract. The stepped reinforcement arrangement in mechanically stabilized earth (MSE) walls is more complicated than the common uniform arrangement design.Afinite element limit analysis (FELA) method combining the advantages of finite element (FE) and limit analysis (LA) methods was used to investigate the influence of stepped reinforcement arrangements on the seismic stability of MSE subjected to vertical and horizontal earthquakes. The pseudo-static FELA method was validated against results from model tests and the limit equilibrium-based (LE) method. The validated numerical model was then used to investigate the seismic stability and failure mechanisms of MSE walls with stepped reinforcement arrangements. Results indicate that multiple slip planes form in reinforced zone and backfills. The stepped reinforcement arrangement can help improve seismic stability. However, excessive increases in reinforcement length toward the top of the wall could have a negative influence on seismic stability, especially in cases of walls with wide reinforcement spacing.

Keywords: failure mechanism; finite element limit analysis; MSE walls; seismic stability; stepped reinforcement arrangement

1. Introduction

Reinforced soil retaining walls (alternatively known as Mechanically Stabilized Earth, MSE walls) are popular in infrastructure applications due to their advantages over conventional walls, including seismic performance, aesthetics, and cost-effectiveness (Berg *et al.* 2009, Derksen *et al.* 2018, Hamrouni *et al.* 2018, Zheng *et al.* 2018, Safa *et al.* 2019). Mirmoazen *et al.* (2021) conducted a numerical investigation on MSE walls subjected to footing loads, where the influence of the inherent anisotropy of the backfill soil was considered. Their find--ings revealed that the coefficient of active earth pressure increased with the anisotropy ratio. Yazdandoust and Daftari (2024) investigated the bearing capacity of back-to-back MSE walls and found that the bearing capacity values were influenced by reinforcement stiffness and soil-reinforcement inter-action, with particular emphasis on the former.Among them, the seismic performance has increasingly drawn attention to researchers in recent years (Matsuo *et al.* 1998, El- Emam and Bathurst 2004, 2007, Bathurst and Hatami 1998, Latha and Krishna 2008, Anastasopoulos *et al.* 2010, Liu *et al.* 2011, Guler *et al.* 2012, Ghanbari *et al.* 3013, Yazdandoust 2017, Alhajj Chehade *et al.* 2021). Yazdandoust *et al.* (2023) presented experimental and analytical results on MSE walls with various configurations and reinforcement types. Their findings indicated that the wall facing exerted a more pronounced influence on yield acceleration as compared to the reinforcement type. Ge *et al.* (2024) examined the seismic stability of MSE walls configured in tiers using the pseudo-static method. Their research revealed that the critical offset distance was sensitive to variations in the soil friction angle and wall height.

Reinforcement lengths are usually uniform along wall height (Berg *et al.* 2009, Mahmood *et al.* 2022). However, nonuniform reinforcement arrangement, especially stepped reinforcement arrangement is also usually adopted in fields in case of the MSE walls constructed on existing slope. For example, many existing embankments were reconstructed to vertical MSE walls with stepped reinforcement arrangement for high-speed train yards after earthquakes in Japan (Tatsuoka 2019). Many model tests have been carried out to investigate the seismic performance of MSE walls with stepped reinforcement arrangement. Ling *et al.* (2005) and Koseki (2012) carried out shaking table tests on MSE walls with extended reinforcement layers at the top of the wall. They found that observed seismic performance of this type wall was better than those without extended reinforcement layers. Panah *et al.* (2015) reported shaking table test results on scaled MSE walls with a stepped

*Corresponding author, Professor
E-mail: bk20090201@my.swjtu.edu.cn
[a]Professor
E-mail: liuweichao@stdu.edu.cn
[b]Professot
E-mail: gtsyang@163.com
[c]Professor
E-mail: chencong0001@139.com

Copyright © 2024 Techno-Press, Ltd.

ISSN: 2005-307X (Print), 2092-6219 (Online)

reinforcement arrangement. They concluded that a stepped reinforcement arrangement in which the length of steps increased from the bottom to the top of the wall could reduce wall displacement significantly. However, the rationality of this stepped reinforcement arrangement for full scale walls is not sure. Besides, the influence of vertical acceleration is not considered in the model tests. Yang *et al.* (2024) conducted numerical simulations on shored MSE walls. They found that the maximum reinforcement loads derived from their numerical method fell within the solutions from the stiffness and simplified methods. Yazdandoust and Daftari (2024) investigated the bearing capacity of back-to-back MSE walls and found that the bearing capacity values were influenced by reinforcement stiffness and soil-reinforcement interaction, with particular emphasis on the former.

Even though model tests could help provide a better understanding of the seismic performance of MSE walls with stepped reinforcement arrangement, pseudo-static design methods are still commonly used due to their practical advantages. However, the geometry of stepped reinforcement arrangements could result in unknown and more complicated failure mechanisms as compared to uniform reinforcement length cases. Since the shape of slip planes need to be assumed before calculating in conventional limit equilibrium (LE) methods, these methods cannot be used under this condition. Besides, boundary conditions and flow rules are not considered in LE methods. On the other hand, the finite element limit analysis (FELA) method provides more rigorous solutions in geotechnical stability analysis in complicated cases using a second-order cone programming (SOCP) and mesh adaptive technology to search the slip planes automatically (Sloan 2013, Krabbenhoft *et al.* 2015). The uses of FELA method in stability analysis of reinforced soil structures have been reported by many researchers (Xie *et al.* 2019, Shiau and Al-Asadi 2020, Fathipour *et al.* 2021a, Xu *et al.* 2020, 2021, Kounlavong *et al.* 2023). Fathipour *et al.* (2023) analyzed the passive and active pseudo-dynamic earth pressures using the FELA method. Their results indicated that foundation elasticity and soil damping were critical factors in pseudo-dynamic analysis. Additionally, Halder and Chakraborty (2023) demonstrated that maximum reinforcement resistance was significantly mobilized when a fully rough interface was assumed between the reinforcement and backfill. However, the application of this method in seismic stability of MSE walls with stepped reinforcement arrangement is scarce. Additionally, previous studies mainly focused on the case of MSE walls subjected on horizontal earthquakes, vertical seismic motions are also significantly pronounced for MSE walls constructed in near-fault regions.

In this paper, a validated FELA method is used to investigate the seismic stability of MSE walls with stepped reinforcement arrangements. Parametric analyses are carried out to investigate the influences that reinforcement design, vertical acceleration, and wall height could have on the predicted yield acceleration and corresponding failure mechanism of MSE walls with different stepped reinforcement arrangements.

2. Methodology and validation

2.1 Methodology

The FELA method combines the advantages of the finite element (FE) and limit analysis (LA) methods to solve stability in irregular geometries and boundary conditions. Besides, the influences of soil-structure interactions and soil materials can also be considered in analysis. The upper bound solution of the FELA method provides a better insight into the corresponding failure mechanism ascompared to the lower bound solution (Sloan 2013, Daset *al.* 2022).

The domain is discretized into linear elements in the FELA method. These elements should enable a kinematically admissible velocity field in a rigorous manner and can effectively model velocity discontinuities along all inter-element edges. The upper-bound solution is formulated as a non-linear optimization problem, wherein the unknowns consist of element stresses, plastic multipliers, and nodal velocities. The objective function to be minimized is the rate of work performed by external forces more the internal power dissipation. Consequently, in accordance with the upper-bound theorem, the unknowns are subject to constraints arising from the velocity boundary conditions, the flow rule, and the yield condition. Thus, the finite element upper-bound solution can be expressed as the following mathematical problem (Krabbenhoft *et al*. 2015).

$$
\begin{aligned}
&\text{minimize} \quad \boldsymbol{\sigma}^{\mathrm{T}}\overline{\mathbf{B}}\mathbf{u} - \int_{A_1}\mathbf{t}^{\mathrm{T}}\mathbf{u}dA - \int_{V}\mathbf{g}^{\mathrm{T}}\mathbf{u}dV \\
&\text{subject to} \\
&\quad \mathbf{A}\mathbf{u} = \mathbf{b} \quad \text{Velocity boundary conditions} \\
&\quad \overline{\mathbf{B}}^{e}\mathbf{u}^{e} = \dot{\boldsymbol{\lambda}}^{e}\nabla f(\boldsymbol{\sigma}^{e}) \quad \text{Flow rule condition for element e} \\
&\quad f(\boldsymbol{\sigma}^{e}) \le \mathbf{0} \quad \text{Yield condition for element e} \\
&\quad \dot{\boldsymbol{\lambda}}^{e} \ge 0 \quad \text{Plastic mutiplier for element e} \\
&\quad \dot{\lambda}^{e} f(\boldsymbol{\sigma}^{e}) = 0 \quad \text{Consistency condition for element e}
\end{aligned}
\tag{1}
$$

where $\boldsymbol{\sigma}$ is a global vector of stresses; $\overline{\mathbf{B}}$ is a global strain–displacement matric; $\mathbf{u}$ is a global vector of nodal velocities; $\mathbf{t}$ is a vector of known tractions; $\mathbf{g}$ is a vector of fixed body forces; $\bar{\boldsymbol{B}}^{e}$is the strain-displacement matrix of element e; $\mathbf{u}^{e}$ is the vector of nodal velocities of element e; $\dot{\boldsymbol{\lambda}}^{e}$ is the vector of plastic multiplier of element e; $\mathbf{A}$ is a metric of constants, $\mathbf{b}$ is a vector of constants; and $f(\boldsymbol{\sigma}^{e})$ is the yield condition of element e, respectively.

The associated flow rule is employed in this study, and the soils are assumed to be Mohr-Coulomb materials. Besides, Second-Order Cone Programming (SOCP) is utilized to obtain the upper-bound solutions. Details about the FELA method used in this study can be referred to Krabbenhoft et al. (2015) and Xu etal. (2021). The FELA method implemented in the software of OPTUMG2 was used for the analysis in this study.

2.2 Validation

The FELA method used in this study was validated in a series of previous studies by the authors in cases of one and

Table 1 Parametric values used in the numerical method invalidation

Parameter	Case 1 (Watanbe *et al.* 2003)		Case 2 (Yazdandoust *et al.* 2024)	Case 3 (Panah *et al.* 2015)	
	a	b	/	a	b
Soil unit weight, γ (kN/m^3)	15.9	15.9	14.9	18	18
Soil friction angle, ϕ (^{o})	51	51	47	40	40
Reinforcement length, l (m)	0.2	0.2 /0.45 / 0.8	0.6*H*/0.35H	0.5/0.7 /0.9	0.5/0.7
Reinforcement vertical spacing, s_V (m)	0.05	0.05	0.075	0.075	0.075
Reinforcement tensile strength, T (kN/m)	10	10	1.23	2.39	2.39
Soil-reinforcement interface shear strength coefficient,f	0.75	0.75	2/3	0.7	0.7
Wall height, H (m)	0.5	0.5	0.9	0.8	0.8

Table 2 Predicted k_y from different methods

		1-a	1-b	2
	Wall geometry	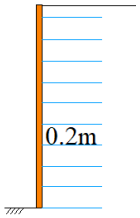	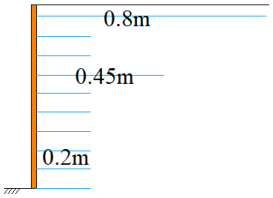	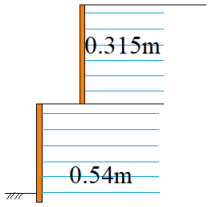
ky	From model tests	0.552	0.670	0.70[1]/0.82[2]/0.87[3]
	From LE method	0.500	0.572	0.65[1]/0.71[2]/0.82[3]
	From FELA method	0.455	0.688	0.72[1]/0.84[2]/0.90[3]

two-tiered MSE walls and back-to-back MSE walls. Details about the wall facing and interaction between soil and reinforcement in numerical model can be referred to Xu *et al.* (2020, 2021).

To the best of the authors' knowledge, no studies on seismic stability of full-scaled MSE walls with stepped reinforced arrangement have been reported. So the FELA method was further validated in this section by comparing numerical results with scaled shaking table test results reported by Watanbe *et al.* (2003), Yazdandoust *et al.* (2024) and Panah *et al.* (2015).

Watanbe *et al.* (2003) carried out shaking table tests on 0.5m heigh MSE walls. They also compared the yield acceleration from model tests with those from design guidelines in Japan (RTRI 2006). The reinforcement length was 0.2 m in the uniform reinforcement length case and two extended layers with length of 0.45 m and 0.8 m, respectively were used in the comparative case. An irregular excitation was used as the base accelerations, which was increased at increments of 100gals until the model walls deformed significantly.Yazdandoust *et al.* (2024) presented both experimental and numerical results on tiered MSE walls. The walls were constructed with two tiers of equal height and three offset distances, as detailed in Table 1. Each wall was 0.9 meters high, with reinforcement length in the lower and upper tiers measuring 0.6 times and 0.35 times the total wall height, respectively. The walls were subjected to a series of harmonic excitations with a frequency of 5 Hz. Panah *et al.* (2015) investigated the influence of reinforcement arrangement on 0.8 m heigh MSE walls with precast concrete panels using shaking table tests. The model walls were reinforced by polymeric strips but with different length along wall height. The acceleration amplitude increased with the increment steps of 0.05 g at each step.

Parameters used in numerical simulations were consistent with those from model tests as listed in Table 1.

Values of the yield acceleration from model tests and different mehtods are listed in Table 2. The yield acceleration resported by Watanbe *et al.* (2003) is defined as an acceleration, beyond which the displacement of the wall increases suddenly (Watanbe et al. 2003). Results in Table 2 indicate that ky from both FELA and LE methods shows good agreement with those from model tests. ky in Case 1-b is larger as compared to that in Case 1-a due to the two extended reinforcement layers as shown in Table 1. ky from the FELA method is slightly smaller than that from the LE method in Case 1-a, and it is closer to the result from the model test in Case 1-b with a more complicated reinforcement arrangement. This can be attributed to the automatically slip planes searching technique adopted in the FELA method. However, the shape of slip planes is assumed before calculation in the FE method

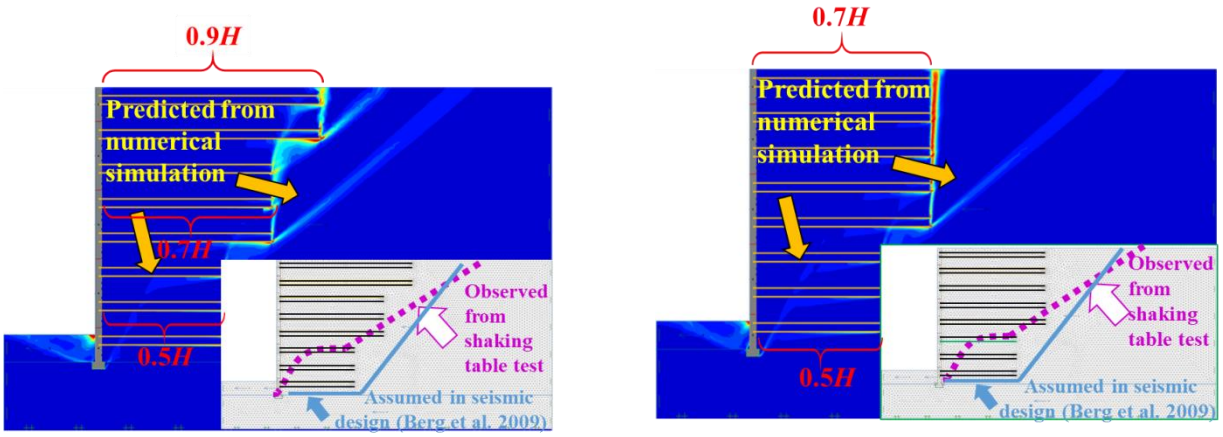

(a) (b)

Fig. 1 Slip planes from different methods: (a) Case 2-a and (b) Case 2-b

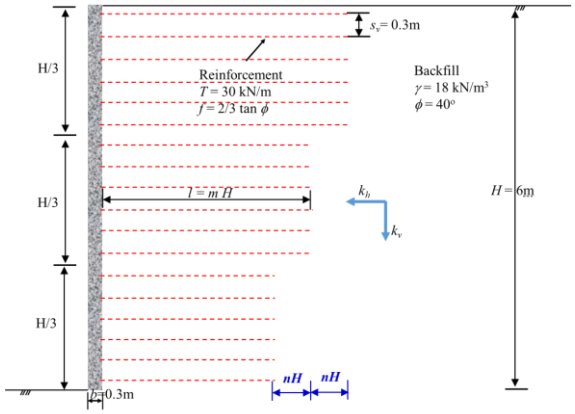

Fig. 2 Schematic cross section of control MSE numerical model

The predicted values of k_y presented in Table 2 also indicate that the results obtained from the FELA method in this study were larger than those from the FE method reported by Yazdandoust *et al*. (2024), and were closer to the measured results. This observed accuracy can be attributed to the application of the upper bound theorem utilized in the FELA method.

Since the values of yield acceleration were not reported by Panah *et al*. (2015), only the shape of slip planes is used for comparison. Fig. 1 shows the observed and predicted slip planes in Case 2 from model tests (Panah *et al.* 2015) and the FELA method, respectively. As shown in Fig. 1, the shape of slip planes is more complicated than that assumed in current seismic design guidelines (Berg *et al.* 2009), where the sip planes are along the base of the reinforced zone and extend upwards to the backfill surface in external stability analysis. However, results from the model tests indicate that slip planes occur in both reinforced zone and backfills, originating from the facing toe and extending upwards to the back of the reinforced zone and further to the backfill surface behind the reinforced zone. The complicated shape of slip planes can be better captured using the FELA method. Results in Fig. 1 from the FELA method also indicate that additionally slip planes at the back of the reinforced zone are also observed.

3. Parametric analysis

Parametric analyses were carried out using the validated FELA numerical model to investigate the pseudo-static stability of MSE walls with stepped reinforcement arrangement. The geometry and parameters of the control MSE numerical model is shown in Fig. 2, where the reinforcement arrangement is step-shaped and m=0.7. The backfill was modelled as Mohr-Column material. The wall facing presents full-height rigid facings commonly used in railway engineering (Tatsuoka 2019). So the facing was modelled as linear elastic materials and facing local failure was not considered in this study. The wall height was divided into three equal segments with stepped reinforcement arrangements. The length of each reinforcement layer in these three segments from the bottom to the top of the wall is (m-n)H, mH, and (m+n)H, respectively.

It should be noted that pull-out failure and rupture failure were both considered in this study.The reinforcement-soil interaction was modeled using a coefficient of 2/3 to simulate potential pull-out failure, while the tensile strength was set at 30 kN/m for the control wall to simulate potential rupture failure. Besides, although some studies have demonstrated the significance of the inherent anisotropy of backfill soil (Mirmoazen *et al.* 2021), this study assumed the backfill soil to be isotropic, consistent with previous numerical investigations (Sloan 2013, Zheng *et al.* 2018, Xu *et al.* 2021).

3.1 Influence of reinforcement length

Fig. 3 shows the variations of yield acceleration coefficient, k_y with n for MSE walls with different reinforcement length, l, reinforcement tensile strength, T, and vertical acceleration (i.e., k_v/k_h). The parameters are the same with the control model wall shown in Fig. 2

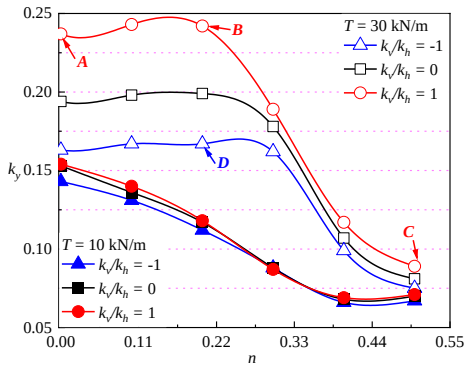

(a)

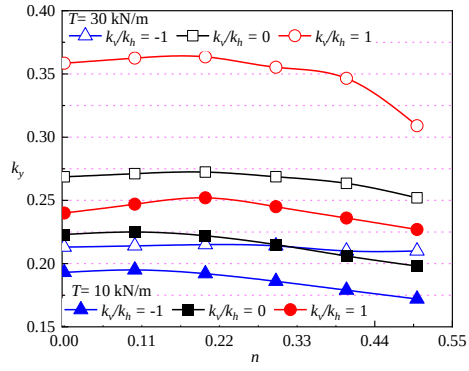

(b)

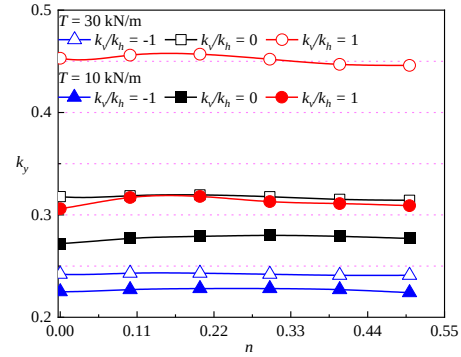

(c)

Fig. 3 Variations of ky with n for MSE with different reinforcement length: (a) $l = 0.5H$, (b) $l = 0.7H$ and (c) $l = 0.9H$

except those mentioned in this section. Results in Fig. 3(a) indicate that when $T = 30$ kN/m, ky increases slightly with n until a peak value, beyond which n has a negative influence on ky. This behavior can be attributed to the competing influences of vertical stress acting on the reinforcements and horizontal earth pressure. Results in Fig. 3(a) also indicate that a similar trend is observed for the cases when kv/kh =0 and -1. However, the changes in trend are less significant under these conditions. It means that excessive increases in reinforcement length toward the top of the wall in a stepped reinforcement design, especially when $n \geq 0.22$ would negatively impact its seismic stability, especially when the vertical acceleration acts downwards. It should be noted that

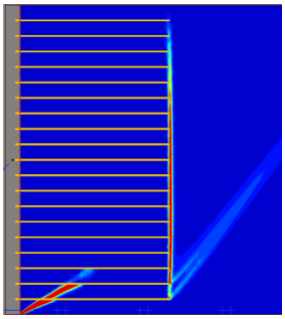

(a)

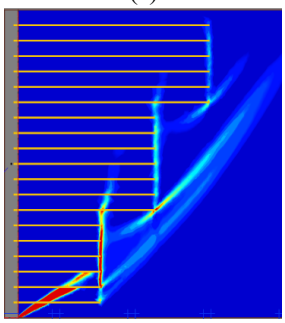

(b)

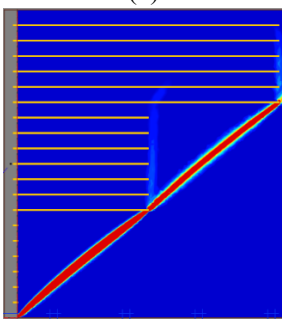

(c)

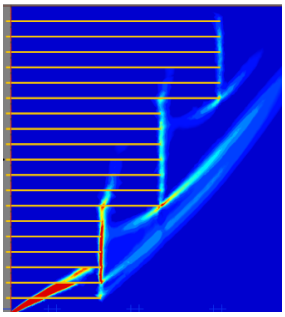

(d)

Fig. 4 Slip planes at selected points from Fig. 3: (a) Point *A,* (b) Point *B,* (c) Point *C* and (d) Point *D*

the total reinforcement length is constant in different kv/kh cases, i.e., lengthening reinforcement in the top part of the wall in a stepped design means decreases of reinforcement length in the bottom part of the wall as shown in Fig. 2. The influence of vertical acceleration on ky is more obvious in case of $T = 30$ kN/m as compared to that in case of $T = 10$ kN/m. Besides, it also can be found that ky decreases with n when weak reinforcement is used (i.e., $T = 10$ kN/m in Fig. 3(a)).

Results in Figs. 3(b) and 3(c) are similar to that in Fig. 3(a). They all indicate that k_y increases with k_v/k_h. Although the variation of k_y with n is still slightly humped-shaped as shown in Figs. 3(b) and 3(c), the sharp decreases in k_y at larger n values is not observed. Results in Figs. 3(b) and 3(c) also indicate that the influence of n on k_y decreases with l. So a stepped reinforcement design is not necessary when reinforcements are longer than $0.7H$.

Fig. 4 shows slip planes at selected points from Fig. 3(a). The slip planes in Fig. 4 are determined by the shear dissipations, which is an indicator to evaluate the energy in FELA method and a larger value means potential failure. A two-part wedge geometry is observed in Fig. 4(a), which is consistent with observations reported in previous numerical and experiment studies (Bathurst and Hatami 1998, Watanbe *et al.* 2003, Liu *et al.* 2011).

Different from the assumption of the slip planes assumed in external stability design guidelines (Berg *et al.* 2009), where they are along the surface of the foundation, the slip planes in Fig. 4(a) are intercepted by several reinforcement layers at the bottom of the reinforced zone. The slip planes in Fig. 4(b) form farther away from the wall facing as compared to that in Fig. 4(a), leading to a larger value of k_y at Point B in Fig. 3(a). When n increases to 0.5 (i.e., Point C in Fig. 3(a)), corresponding slip planes shown in Fig. 4(c) are out of the reinforced zone, which means that reinforcement contributes less to seismic stability, leading to a smaller k_y at Point C. The shape of slip planes at Point D (i.e., Fig. 4(d)) is similar to that at Point B (i.e., Fig. 4(b)). However, since the upwards vertical acceleration at Point D results in less vertical stress acting on reinforcement layers as compared to that at Point B, less reinforcement force is mobilized in Fig. 4(d), corresponding to a smaller k_y at Point D in Fig. 3(a). It should be noted that when the downwards vertical acceleration is large enough, its influence on horizontal pressure acting on the wall would large than that because of the increase in mobilized reinforcement force, which means that it has a negative influence on seismic stability under this condition.

3.2 Influence of reinforcement vertical spacing

Fig. 5 shows the variations of k_y with n for MSEwalls with different reinforcement vertical spacing, s_v. The parameters are the same with those in Fig. 2 except those mentioned in this section. Results in Fig. 5(a) indicate that when k_v/k_h = -1 and $s_v \leq 0.2$ m, k_y in a stepped reinforcement design (i.e., $n > 0$) is consistently larger than that in a common uniform reinforcement length design (i.e., $n = 0$). Therefore, using a stepped reinforcement design is an efficient way to increase seismic stability in cases where reinforcement is tightly spaced. However, when $s_v > 0.2$ m, results in Fig. 5(a) show a critical n value (i.e., pink points in Fig. 5(a)) beyond which excessive increases in reinforcement length toward the top of the wall would decrease the seismic stability when the total reinforcement length is constant. Additionally, this critical value is greater

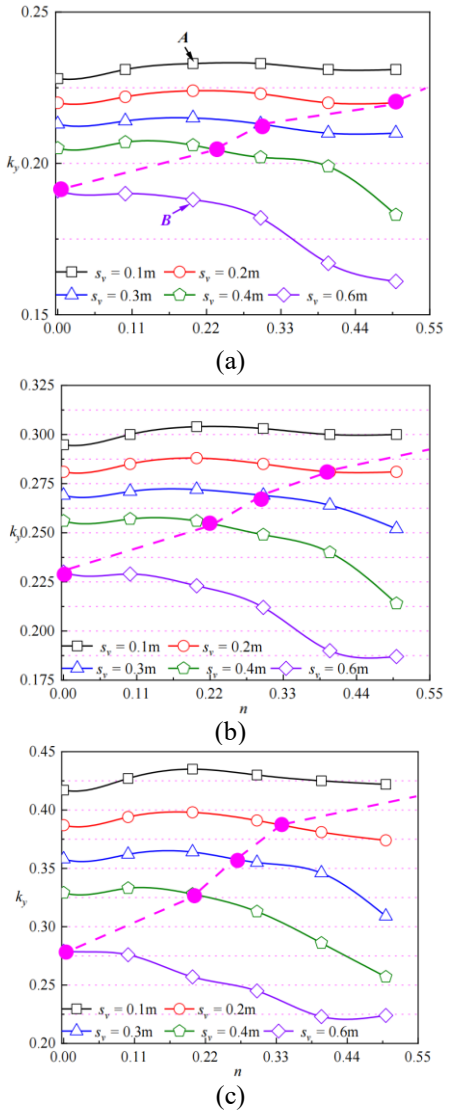

Fig. 5 Variations of k_y with n for MSE walls with different vertical spacing, s_v : (a) k_v/k_h = -1, (b) k_v/k_h = 0 and (c) k_v/k_h = 1

for MSE walls with smaller vertical spacing,s_v. Specially, when s_v increases to a larger value of 0.6 m, k_y decreases with n within the parameters examined in this study. So in cases of wide reinforcement spacing, a common used uniform reinforcement length design can achieve a better seismic stability as compared to those using a stepped reinforcement arrangement design.

k_y values in Figs. 5(b) and 5(c) are larger than those in Fig. 5(a). Besides, the critical n value decreases with k_v/k_h. For instance, the critical n value in Figs. 5(a) to 5(c) for s_v = 0.2 m are 0.5, 0.4, and 0.34, respectively. It means that although a stepped reinforcement design can achieve a larger k_y, the reinforcement length in the top part of the wall should not be too long, especially when larger downwards vertical acceleration acts on the wall. Finally, results in Fig. 5 provide a solution to select an optimum n value in stepped reinforcement arrangement design for walls with different reinforcement vertical spacing.

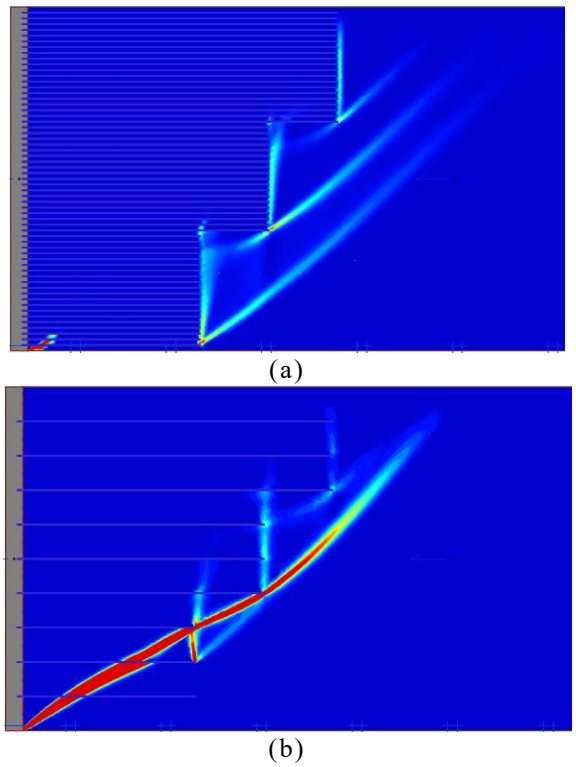

Fig. 6 Slip planes at selected points from Fig. 5: (a) Point A and (b) Point B

Fig. 6 shows slip planes at selected points from Fig. 5. Results in Fig. 6(a) indicate that multiple slip planes form in backfill, which means a greater dissipation of internal energy in MSE walls under earthquakes to maintain the stability of the wall (Sloan 2013), leading to a greater k_y value at Point A in Fig. 5(a). The inclination of slip planes in reinforced zone is steeper in Fig. 6(b) as compared to that in Fig. 6(a) due to the fact that the wide spacing reinforcement cannot prevent the generating of slip planes, leading to a smaller k_y value at Point B in Fig. 5(a).

3.3 Influence of wall height

Fig. 7 shows the variations of k_y with n for MSE walls with different wall height, H. The parameters are the same with the control model wall shown in Fig. 2 except those mentioned in this section. Results in Fig. 7(a) indicate that k_y values are comparable to those in Fig. 3(b) for 6 m-high walls. And they both indicate that the influence of stepped reinforcement arrangement design on seismic design of MSE wall is more significant when the vertical acceleration is downwards (i.e., k_v/k_h >0). Since the vertical stress acting on reinforcement is smaller in cases of k_h/k_v= 0 and -1, the humped-shaped distributions of k_y are not observed. k_y values in Fig. 7(b) for taller walls are smaller than those in Figs. 3(b) and 7(a). The reason can be attributed that more horizontal pressure acting on the wall when H= 9 m as compared to that when H =3 and 6 m. Besides, results in Fig. 7(b) also indicate that overall, a stepped reinforcement arrangement design would have a negative influence on seismic stability of taller walls.

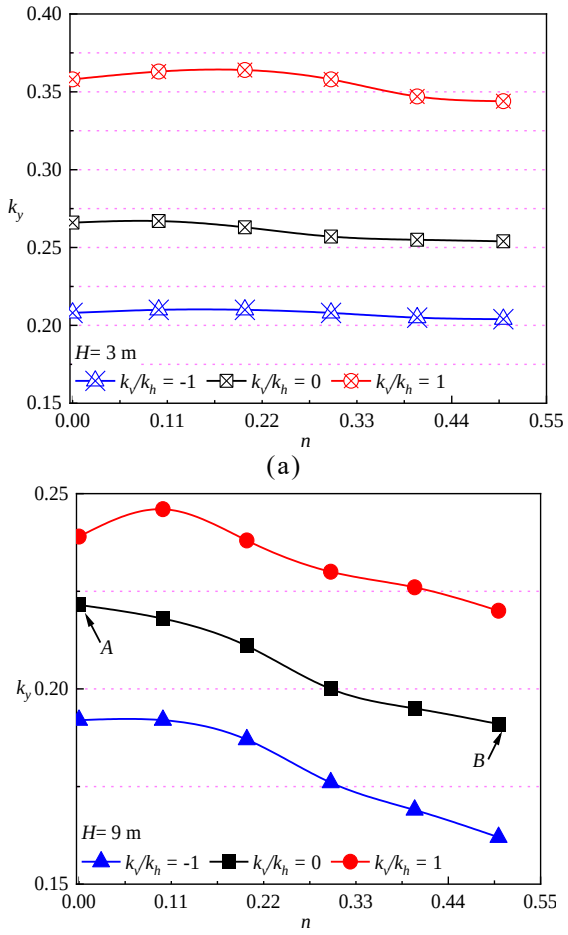

Fig. 7 Variations of k_y with n for walls with different wall height: (a) H = 3 m and (b) H = 9 m

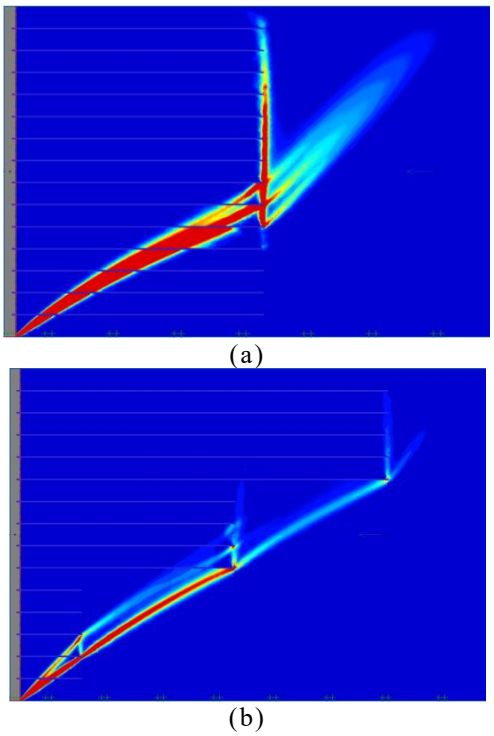

Fig. 8 Slip planes at selected points from Fig. 7: (a) Point A and (b) Point B

Fig. 8 shows slip planes at selected points from Fig. 7(b) for the cases of n = 0 and 0.5. The slip planes corresponding to Point A in Fig. 7(b) are mainly located in the retained zone, part of them intercepting reinforcement layers toward the bottom of the wall and others along the back of the reinforced zone, forming a two-part wedge geometry. It means that multiple failure mechanisms develop under earthquakes, rather than completely external or internal failure mechanisms as that assumed in current seismic design (Bergetal 2009). Since reinforcements contribute less in Fig. 8(b) (i.e.m fewer reinforcement layers intersect with slip planes toward the bottom of the wall), the k_y value at Point B in Fig. 7(b) is smaller as compared to that at Point A.

4. Conclusions

In this study, the pseudo-static stability of MSE walls with stepped reinforcement arrangements was investigated using the FELA method. The analysis considered the velocity boundary condition, yield condition, and consistency condition. SOCP and mesh-adaptive technology were employed to obtain the upper-bound solutions and corresponding slip planes. The main conclusions drawn are as follows:

• The predicted results of the yield acceleration coefficient from the FELA method are closer to those obtained from scaled shaking table tests compared to results from LE methods. Multiple slip planes form within the reinforced zone and backfill, with the shape of these slip planes in MSE walls being more complex than currently assumed in seismic design guidelines. The FELA method is more effective in predicting yield acceleration and corresponding failure mechanisms in walls with stepped reinforcement arrangements.

• The influence of stepped reinforcement arrangements on seismic stability diminishes as the reinforcement length increases. The yield acceleration coefficient, k_y increases with the ratio of vertical acceleration to horizontal acceleration, k_v/k_h. However, the influence of k_v/k_h on k_y decreases with reinforcement ultimate strength. This can be attributed to the competing effects of vertical stress on reinforcements and the tensile strength of the reinforcement.

• Employing stepped reinforcement arrangements can lead to a higher k_y, particularly for MSE walls with closely spaced reinforcement lengths. However, since the reinforcement length in the lower part of the wall significantly influences sliding stability, an excessive increase in reinforcement length toward the top of the wall may negatively impact seismic stability when the total reinforcement length is constant.

• The stepped reinforcement design is more advantageous for shorter walls (i.e., H =3 m and 6 m) compared to taller walls (i.e., H =9 m) within the parameters analyzed in this study. The yield acceleration coefficient k_y decreases with n for tall walls, as reinforcements located toward the bottom of the wall contribute less to seismic stability.

The effects of wall and backfill stiffness were not considered in this study, consistent with conventional LA methods. To analyze the influence of stiffness on the stability and deformation of reinforced structures, the authors employed the multiplier elastoplastic analysis method in previous studies (Xu *et al.* 2022), which integrated the advantages of elastoplastic analysis and FELA to evaluate the performance of reinforced slopes under footing loads. Other previous stuies also indicated the imorpance of the wall and backfill stiffness in performance analysis of MSE walls (Fathipour *et al.* 2020, 2021b, c, 2022, 2023). So a further future numeirical study is needed.

Acknowledgments

The research described in this paper was financially supported by National Key R&D Program of China (NO.2022YFE0104600), Natural Science Foundation of Hebei Province (NO.E2024210145) and National Natural Science Foundation of China (NO. 52108331).

References

Alhajj Chehade, H., Dias, D., Sadek, M., Jenck, O. and Hage Chehade, F. (2021), "Pseudo-static analysis of reinforced earth retaining walls", *Acta Geotech.*, **16**(7), 2275-2289. https://doi.org/10.1007/s11440-021- 01148-2.

Anastasopoulos, I., Georgarakos, T., Georgiannou, V., Drosos, V. and Kourkoulis, R. (2010), "Seismic performance of bar-mat reinforced-soil retaining wall: Shaking table testing versus numerical analysis with modified kinematic hardening constitutive model", *Soil Dyn. Earthq. Eng.*, **30**(10), 1089-1105. https://doi.org/10.1016/j.soildyn.2010.04.020.

Bahmani Tajani, S., Fathipour, H., Payan, M., Jamshidi Chenari, R. and Senetakis, K. (2023), "Temperature-dependent lateral earth pressures in partially saturated backfills", *Eur. J. Environ. Civ. En.*, **27**(10), 3064-3090. https://doi.org/10.1080/19648189.2022.2125911.

Bathurst, R.J. and Hatami, K. (1998), "Seismic response analysis of a geosynthetic-reinforced soil retaining wall", *Geosynth. Int.*, **5**(1-2), 127-166. https://doi.org/10.1680/gein.5.0117.

Benmeddour, D., Mellas, M., Frank, R., and Mabrouki, A. (2012), "Numerical study of passive and active earth pressures of sands", *Comput. Geotech*., **40**, 34-44. https://doi.org/10.1016/j.compgeo.2011.10.002.

Berg, R.R., Christopher, B.R. and Samtani, N.C. (2009), *Design and Construction of Mechanically Stabilized Earth. Walls and. Reinforced Soil Slopes*, Volume 1, Publication No. FHWA-NHI-10-024, Federal Highway Administration, Washington, DC, USA.

Choudhury, D. and Singh, S. (2006), "New approach for estimation of static and seismic active earth pressure", *Geotech. Geol. Eng.*, **24**(1), 117-127. https://doi.org/10.1007/s10706-004-2366-x.

Das, S., Halder, K. and Chakraborty, D. (2022), "Seismic bearing capacity of shallow embedded strip footing on rock slopes", *Geomech. Eng.*, **30**(2), 123-129. https://doi.org/10.12989/gae.2022.30.2.123.

Derksen, J., Ziegler, M., Detert, O. and Hangen, H. (2018), "Analysis of bearing capacity of reinforced retaining structures", *Proceedings of the 11th International Conference on Geosynthetic*s, Seoul, Korea, September.

El-Emam, M.M. and Bathurst, R.J. (2004), "Experimental design, instrumentation and interpretation of reinforced soil wall response using a shaking table", *Int. J. Phys. Model Geo*.,

4(4), 13-32. https://doi.org/10.1680/ijpmg.2004.040402.

El-Emam, M.M. and Bathurst, R.J. (2007), "Influence of. reinforcement parameters on the seismic response of reduced-scale reinforced soil retaining walls", *Geotext. Geomembranes*, **25**(1), 33-49. https://doi.org/10.1016/j.geotexmem.2006.09.001.

Fathipour, H., Siahmazgi, A.S., Payan, M. and Chenari, R.J. (2020), "Evaluation of the lateral earth pressure in unsaturated soils with finite element limit analysis using second-order cone programming", *Comput. Geotech*., **125**, 103587. https://doi.org/10.1016/j.compgeo.2020.103587.

Fathipour, H., Payan, M. and Chenari, R.J. (2021a), "Limit analysis of lateral earth pressure on geosynthetic- reinforced retaining structures using finite element and second-order cone programming", *Comput. Geotech*., **134**, 104119. https://doi.org/10.1016/j.compgeo.2021.104119.

Fathipour, H., Payan, M., Jamshidi Chenari, R. and Senetakis, K. (2021b), "Lower bound analysis of modified pseudo-dynamic lateral earth pressures for retaining wall-backfill system with depth-varying damping using FEM-Second order cone programming", *Int. J. Numer. Anal. Methods Geomech*., **45**(16), 2371-2387. https://doi.org/10.1002/nag.3269.

Fathipour, H., Siahmazgi, A.S., Payan, M., Veiskarami, M. and Jamshidi Chenari, R. (2021c), "Limit analysis of modified pseudo-dynamic lateral earth pressure in anisotropic frictional medium using finite-element and second-order cone programming", *Int. J. Geomech.*, **21**(2), 04020258. https://doi.org/10.1061/(ASCE)GM.1943-5622.0001924.

Fathipour, H., Tajani, S.B., Payan, M., Chenari, R.J. and Senetakis, K. (2022), "Influence of transient flow during infiltration and isotropic/anisotropic matric suction on the passive/active lateral earth pressures of partially saturated soils", *Eng. Geol*., **310**, 106883. https://doi.org/10.1016/j.enggeo.2022.106883.

Fathipour, H., Safardoost Siahmazgi, A., Payan, M., Jamshidi Chenari, R. and Veiskarami, M. (2023), "Evaluation of the active and passive pseudo-dynamic earth pressures using finite element limit analysis and second-order cone programming", *Geotech. Geol. Eng.*, **41**(3), 1921-1936. https://doi.org/10.1007/s10706-023-02381-0

Ge, B., Fei Z. and Shuang S. (2024), "Seismic analysis of geosynthetic-reinforced soil walls in tiered configuration". *Geotext. Geomembranes*, **52**(5), 1072-1085. https://doi.org/10.1016/j.geotexmem.2024.07.004.

Ghanbari, A., Khalilpasha, A., Sabermahani, M. and Heydari, B. (2013), "An analytical technique for estimation of seismic displacements in reinforced slopes based on horizontal slices method (HSM)", *Geomech. Eng.*, **5**(2), 143-164. https://doi.org/10.12989/gae.2013.5.2.143.

Guler, E., Cicek, E., Demirkan, M.M. and Hamderi, M. (2012), "Numerical analysis of reinforced soil walls with granular and cohesive backfills under cyclic loads", *B. Earthq. Eng*., **10**(3), 793-811. https://doi.org/10.1007/s10518-011-9322-y

Halder, K/ and Chakraborty, D. (2023), "Estimation of seismic active earth pressure on reinforced retaining wall using lower bound limit analysis and modified pseudo-dynamic method", *Geotext. Geomembranes*, **51**(1), 100-116. https://doi.org/10.1016/j.geotexmem.2022.10.001

Hamrouni, A., Dias, D. and Sbartai, B. (2018), "Reliability analysis of a mechanically stabilized earth wall using the surface response methodology optimized by a genetic algorithm", *Geomech. Eng*., **15**(4), 937-945. https://doi.org/10.12989/gae.2018.15.4.937.

Hu, W., Zhu, X., Zeng, Y., Liu, X. and Peng, C. (2022), "Active earth pressure against flexible retaining wall for finite soils under the drum deformation mode", *Sci. Rep*., **12**(1), 497. https://doi.org/10.1038/s41598-021-04411-4.

Koseki, J. (2012), "Use of geosynthetics to improve seismic performance of earth structures", *Geotext. Geomembranes*, **34**, 51-68. https://doi.org/10.1016/j.geotexmem.2012.03.001.

Kounlavong, K., Chavda, J.T., Jamsawang, P. and Keawsawasvong, S. (2023), "Stability analysis of buried pipelines under combined uplift and lateral forces using FELA and ANN", *Appl. Ocean Res.*, **135**, 103568. https://doi.org/10.1016/j.apor.2023.103568.

Krabbenhoft, K., Lyamin, A. and Krabbenhoft, J. (2015), *Optum computational engineering (OptumG2)*. Computer software. https://www. optumce. com.

Latha,G.M. and Krishna, A.M. (2008), "Seismic response of reinforced soil retaining wall models: influence of backfill relative density", *Geotext. Geomembranes*, **26**(4), 335-349. https://doi.org/10.1016/j.geotexmem.2007.11.001:

Ling, H.I., Mohri, Y., Leshchinsky, D., Burke, C., Matsushima, K. and Liu, H. (2005), "Large-scale shaking table tests on modular-block reinforced soil retaining walls", *J. Geotech. Geoenviron. Eng*., **131**(4), 465-476. https://doi.org/10.1061/(ASCE)1090-0241(2005)131: 4(465)

Liu, H., Wang, X. and Song, E. (2011), "Reinforcement load and deformation mode of geosynthetic- reinforced soil walls subject to seismic loading during service life", *Geotext. Geomembranes*, **29**(1), 1-16. https://doi.org/10.1016/j.geotexmem.2010.06.003.

Mahmood, Z., Qureshi, M.U., Memon, Z.A. and Imran Latif, Q.B.A. (2022), "Ultimate limit state reliability-based optimization of MSE wll considering external stability", *Sustainability-Basel*, **14**(9), 4968. https://doi.org/10.3390/su14094968.

Matsuo, O., Yokoyama, K., and Saito,Y. (1998), "Shaking table tests and analyses of geosynthetic-reinforced soil retaining walls", *Geosynth. Int.*, **5**(1-2), 97-126. https://doi.org/10.1680/gein.5.0116.

Mirmoazen, S.M., Lajevardi, S.H., Mirhosseini, S. M., Payan, M., and Chenari, R. J. (2021), "Active lateral earth pressure of geosynthetic-reinforced retaining walls with inherently anisotropic frictional backfills subjected to strip footing loading", *Comput. Geotech.*, 137, 104302. https://doi.org/10.1016/j.compgeo.2021.104302

Mirmoazen, S. M., Lajevardi, S. H., Mirhosseini, S. M., Payan, M., and Jamshidi Chenari, R. (2022), "Limit analysis of lateral earth pressure on geosynthetic-reinforced retaining structures subjected to strip footing loading using finite element and second-order cone programming", *Iran. J. Sci. Technol. Trans. Civ. Eng*., **46**, 3181-3192. https://doi.org/10.1007/s40996-021-00793-7.

Pain, A., Choudhury, D. and Bhattacharyya, S.K. (2015), "Seismic stability of retaining wall–soil sliding interaction using modified pseudo-dynamic method", *Geotech. Lett.*, **5**(1), 56-61. https://doi.org/10.1680/geolett.14.00116

Panah, A.K., Yazdi, M. and Ghalandarzadeh, A. (2015), "Shaking table tests on soil retaining walls reinforced by polymeric strips", *Geotext. Geomembranes*, **43**(2), 148-161. https://doi.org/10.1016/j.geotexmem.2015.01.001.

Payan, M., Fathipour, H., Hosseini, M., Chenari, R.J. and Shiau, J. S. (2022), "Lower bound finite element limit analysis of geo-structures with non-associated flow rule", *Comput. Geotech.*, 147, 104803. https://doi.org/10.1016/j.compgeo.2022.104803.

Railway Technical Research Institute, (2006), *Design standard for railway earth structures*, Railway Technical Research Institute, Japan

Safa, M., Maleka, A., Arjomand, M.A., Khorami, M. and Shariati, M. (2019), "Strain rate effects on soil- geosynthetic interaction in fine-grained soil" . *Geomech. Eng*., **19**(6), 533-541. https://doi.org/10.12989/gae.2019.19.6.533.

Shiau, J. and Al-Asadi, F. (2020), "Stability analysis of twin circular tunnels using shear strength reduction method", *Geotech. Lett.*, **10**(2), 311-319.

https://doi.org/10.1680/jgele.19.00003.
Sloan, S.W. (2013), "Geotechnical stability analysis", *Geotechnique*, **63**(7), 531-571. https://doi.org/10.1680/geot.12.RL.001.
Tatsuoka, F. (2019), "Geosynthetic-reinforced soil structures for railways and roads: development from walls to bridges", *Innov Infrastruct So*., **4**(1), 1-18. https://doi.org/10.1007/s41062-019-0236-x
Watanbe, K., Munaf, Y., Koseki, J., Tateyama, M. and Kojima, K. (2003), "Behaviors of several types of model retaining walls subjected to irregular excitation", *Soils Found*., **43**(5), 13-2. https://doi.org/10.3208/sandf.43.5_13.
Xie, Y. and Leshchinsky, B. (2015), "MSE walls as bridge abutments: Optimal reinforcement density", *Geotext. Geomembranes*, **43**(2), 128-138. https://doi.org/10.1016/j.geotexmem.2015.01.002.
Xu, P., Hatami, K., Bao, J. and Li, T. (2020), "Bearing capacity and failure mechanisms of two-tiered reinforced soil retaining walls under footing load", *Comput. Geotech.*, **128**, 103833. https://doi.org/10.1016/j.compgeo.2020.103833.
Xu, P., Yang, G., Li, T. and Hatami, K. (2021), "Finite element limit analysis of bearing capacity of footing on back-to-back reinforced soil retaining walls", *Transp. Geotech*., **30**, 100596. https://doi.org/10.1016/j.trgeo.2021.100596.
Xu, P., Li, T., Hatami, K., Yang, G. and Liang, X. (2022), "Finite element limit analysis of load-bearing performance of reinforced slopes using a non-associated flow rule", *Geotext. Geomembranes*, **50**(5), 1020-1035. https://doi.org/10.1016/j.geotexmem.2022.07.002.
Yang, S., Song, S., Zhang, F. and Gao, Y. (2024), "Performance Analysis of Shored Mechanically Stabilized Earth Walls with Wrapped Facing Using Numerical Simulations", *J. Geotech. Geoenviron. Eng.*, **150**(6), 04024045. https://doi.org/10.1061/JGGEFK.GTENG-12058.
Yazdandoust, M. (2017), "Investigation on the seismic performance of steel-strip reinforced-soil retaining walls using shaking table test", *Soil Dyn. Earthq. Eng.*, **97**, 216-232. https://doi.org/10.1016/j.soildyn.2017.03.011
Yazdandoust, M., Jamnani, A.R. and Sabermahani, M. (2023), "The role of wall configuration and reinforcement type in selecting the pseudo-static coefficients for reinforced soil walls". *Geomech. Eng.*, **35**(5), 555-570. https://doi.org/10.12989/gae.2023.35.5.555.
Yazdandoust, M. and Daftari. F. (2024), "Behavior of back-to-back mechanically stabilized earth walls as railway embankments", *Geosynth. Int.*, 1-21. https://doi.org/10.1680/jgein.23.00126.
Yazdandoust, M., Jamnani, A.R. and Sabermahani, M. (2024), "Dynamic evaluation of tiered geogrid mechanically stabilized earth (MSE) walls using shake table test", *Acta Geotech.*, **19**(6), 4139-4165. https://doi.org/10.1007/s11440-023-02171-1.
Zheng,Y., Fox, P.J. and McCartney, J.S. (2018), "Numerical simulation of deformation and failure behavior of geosynthetic reinforced soil bridge abutments", *J. Geotech. Geoenviron. Eng.*, **144**(7), 04018037-04018037. https://doi.org/10.1061/(ASCE)GT.1943-5606.00018.